W. T. Chen
T. F. Flavin

Mechanics of Film Adhesion: Elastic and Elastic-Plastic Behavior

Abstract: A peel test is a useful method for comparing the behavior of various adherends and adhesives. An exact analysis of the mechanics of the peel test would be of great help in the interpretation of test results in terms of the bulk properties of the materials, and of the failure mechanism of the bond. The existing theories of peeling apply to *elastic* peel films, *very thin* elastic or viscoelastic adhesive, and a *rigid* substrate. In many applications the film is metallic, stressed beyond its elastic range; the elasticity of the substrate is often similar to that of the adhesive; and the adhesive may be quite thick compared to the film, or may be wholly absent as in electroplated components. In this paper, the effects of non-elastic behavior of the film are analyzed. Results from the use of computer programs that incorporate an analytical model of steady state peeling are presented and compared with experimental data.

Introduction

In the past two decades there have been extensive developments in the technology and application of adhesives. Some recent monographs and symposium proceedings on this subject are listed in Refs. [1] through [12]. An extensive general bibliography has been prepared by Solomon ([6], Vol. II, p. 62).

Peeling is an often observed mode of adhesive bond failure. It is natural to use as an index of bond quality the force sufficient to progressively separate two adherends by peeling. This force, called the peel force or peel adhesion, is widely used by mechanical and material engineers for joint design and quality control purposes. There are several ASTM (American Society for Testing Materials) standards for peel testing of structural adhesive joints such as the strip-back peel test (D903-49), T peel (D-1876-61), and the climbing drum (D 1781-62).

In 1934, Jacquet [13] reported experiments in which he pulled a thin layer of electrolytic deposit at a 90° angle from the underlying substrate. This test, named after Jacquet, remains the most commonly used industrial test for adhesion in the electroplating industry. An early version of the T peel test was reported in 1938 by Chadwick [14], who used it to evaluate soldered joints under different material property variables and environmental conditions. That the peel force should also be one of the first criteria of quality in the pressure sensitive tape industry is not surprising. Procedures for testing such tape have also been established by the industry (Pressure Sensitive Tape Council Test Method No. 1), ASTM (D 1000-65), and the federal government.

A theoretical analysis of the mechanics of peeling was developed by Spies [15]. He considered the 90° peeling of a thin, flexible elastic strip bonded to a rigid substrate by an elastic layer of adhesive. Spies represented the bonded part of the strip as an elastic beam on an elastic (Winkler) foundation, and the flexible part as an elastica—an elastic beam under large deflection. Similar elastic models have also been independently derived and extended by Bikerman [16], Kaelble [17,18], Jouwersma [19], Yurenka [20], and Saubestre, Durney, Hajdu, and Bastenback [21]. In considering other angles of peeling, Kaelble introduced the idea of cleavage and shear modes of failure. Good correlation has also been found between theory and experiments in the variation of the peel force with peel angle and adhesive thickness. By writing the properties of the adhesive as a function of temperature and strain rate, Kaelble [18] was able to extend the elastic analysis to include viscoelastic peeling; his conclusions are well substantiated, particularly in tests with nonmetallic tapes.

In the elastic analysis, it is implicitly assumed that all of the energy input is used to create a rupture surface in the adhesive. If substantial energy is also expended in the plastic deformation of the flexible adherend, the elastic analysis would no longer be applicable. That the plastic deformation could be very important was early recognized by Spies [15] who introduced an average elastic constant to compensate for the ductile or plastic behavior of aluminum strips. Observing that some aluminum alloys behave like an ideally plastic material, Mylonas

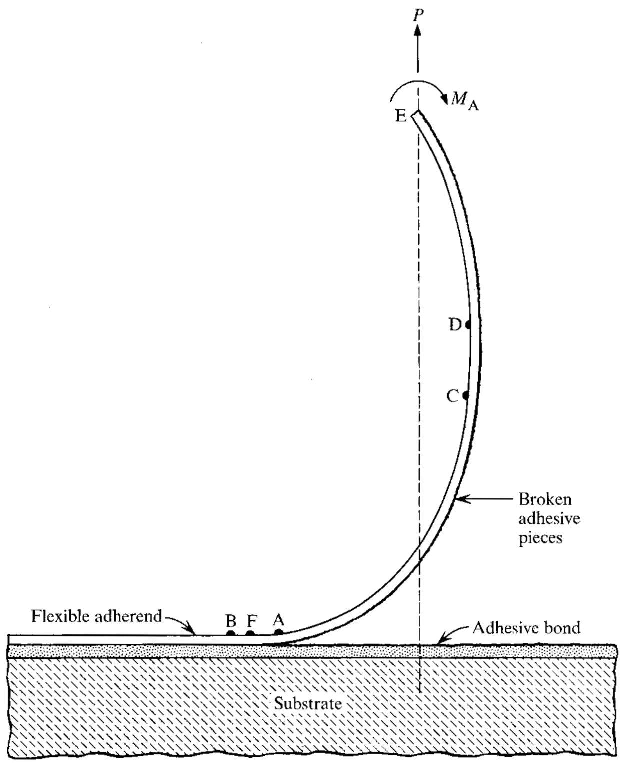

Figure 1 Sketch of 90° peeling.

[22] assumed that the moment at the cleavage point was equal to the limiting plastic moment.

While these ideas have provided insight into the effect of overstressing the flexible adherend in the mechanics of peeling, little is known about the quantitative effects of plasticity in peeling. This paper provides a mathematical model describing the 90° steady state peeling of an elastic-plastic flexible adherend bonded to a rigid substrate by a thin layer of elastic adhesive. From this model, the relationship between peel force and the adhesive cleavage stress may be obtained if the elastic-plastic behavior of the flexible adherend is known. At the elastic limit, this model reduces exactly to the elastic theory in the literature.

Some recent papers by Kaelble [23–25] and Kaelble and Reylek [26], indicate that for some soft, low-modulus adhesives (such as pressure sensitive tapes) the nature of the unbonding process and the stress state in the vicinity of the cleavage region are much more complicated than has been recognized heretofore. However, for the usual structural adhesives, it still appears reasonable to represent the behavior of a thin adhesive layer by a linear Winkler foundation as is demonstrated by Burton, Jones, and Williams [27]. The analysis in this paper is focused on the effect of elastic-plastic behavior of the adherend, and it appears prudent to take the usual elastic peel adhesion theory as the point of departure.

The importance of the peel test to the engineering community is that it is representative of the actual loadings on adhesive bonds. The peel test takes into account not only the critical strength of the bond, but also the ability of the adherend components to apply the load necessary to propagate a crack or a weakness along the bond line. The stress concentration that causes bond failures during peel testing is similar to that produced by differential thermal expansion of the adherends. The susceptibility of the bond depends not only on the bond strength and the elastic properties of the material but also on the ability of that system to relieve stress concentrations by plastic flow of the adherend. That ability might be evidenced by the peel force or peel adhesion. Vazirani [28] has recently shown that peel forces measured in identical samples of the same adhesive, with adherends made from thin aluminum strips of identical dimensions, may differ by a factor of 7 or more depending on whether the aluminum strip has been annealed or work-hardened.* This result has led to a search for a more thorough and basic understanding of the role of the inelastic properties of adherends. Such understanding can be useful in the selection of materials for logic circuit boards and in the assessment of the design of a bonded assembly.

Description of physical system

Figure 1 is a diagrammatic sketch of 90° peeling. The flexible adherend is pulled up vertically at constant speed. The attachment from the adherend to the testing machine is usually designed to eliminate any turning moment, so that the value of M_A (see Fig. 1) is extremely small. One usually finds that the bond failure is cohesive, so that one may see broken pieces of adhesive bonded to the peel parts of the adherends. When the adhesive is a stiff material, its reluctance to conform in bending causes the major portion to remain attached to the stiffer adherend.

At A the adhesive bond fails. In the vicinity of A, say at B, the adherend enters the plastic region. In addition, the adhesive may become plastic in this general vicinity, say at F. Generally speaking, the region of high stress is contained within a very small segment near the bond failure point, so that the distances of B and F from A are of the order of the film thickness. The material along the whole length between A and E has been overstressed during the debonding process so that its relaxed shape will no longer be straight. The force and moment at E provide a straightening action on the adherend to the right of the center line. This straightening action may or may not cause further plastic reverse curvature on the adherend, say in the region CD. If the latter should hap-

*Some other interesting experimental results on plastic yielding in the adherend have recently been published by Duke and Staubridge [29].

pen, the relaxed radii of curvature between E and D and between C and A would be different from each other.

In Fig. 1, the substrate surface is flat. In the vicinity of A the substrate would deform so that the deflection of the adherend at A is the sum of the extensions of the adhesive and the substrate at A.

This is the real picture of peeling. In the theoretical model, however, many simplifying assumptions have to be made. The following list contains the minimum number of assumptions that are usually made in the literature.

1. The substrate adherend is rigid.
2. The peeled strip of film is represented by an "elastica" beam with large deflection.
3. The bonded part of the film-adhesive composite is represented in model form* by a beam on an elastic (Winkler) foundation.
4. Fracture occurs in the adhesive layer when the tensile stress or strain energy density in the adhesive (as computed by Winkler foundation theory) reaches a critical value.
5. The peeled as well as the bonded parts of the film are both very long.
6. The film is initially stress-free.
7. The film is linearly elastic.

• *Elastic theory*

The elastic theory of peeling was originally derived by Spies, and later independently derived and extended by Bikerman, Kaelble and many others. The basic idea as enunciated by Kaelble is shown in Fig. 2(a). He considered the peeling as a quasi-static steady state process in which the fracture point A moved at constant velocity. To an observer moving at the same velocity as A, the same fracture phenomenon would unfold. The bonded part of the peel is considered as a beam on an elastic (Winkler) foundation [30] as shown in Fig. 2(c). The displacement in the beam induced by the moment M and the force P is

$$y = [e^{\beta x}/2\beta^3 EI][\beta M(\cos \beta x + \sin \beta x) + P \sin \omega \cos \beta x], \quad (1)$$

where ω is the angle of peeling,

$$\beta = (Yb/4EIa)^{1/4} = (3Y/Eah^3)^{1/4},$$

Y and E are Young's moduli of adhesive and film, respectively, a is the adhesive thickness, h is one-half the film thickness, b is the film width, and I is the moment of inertia of the film strip.

*A critical survey of elastic foundation theories has recently been given by Hetényi [30].

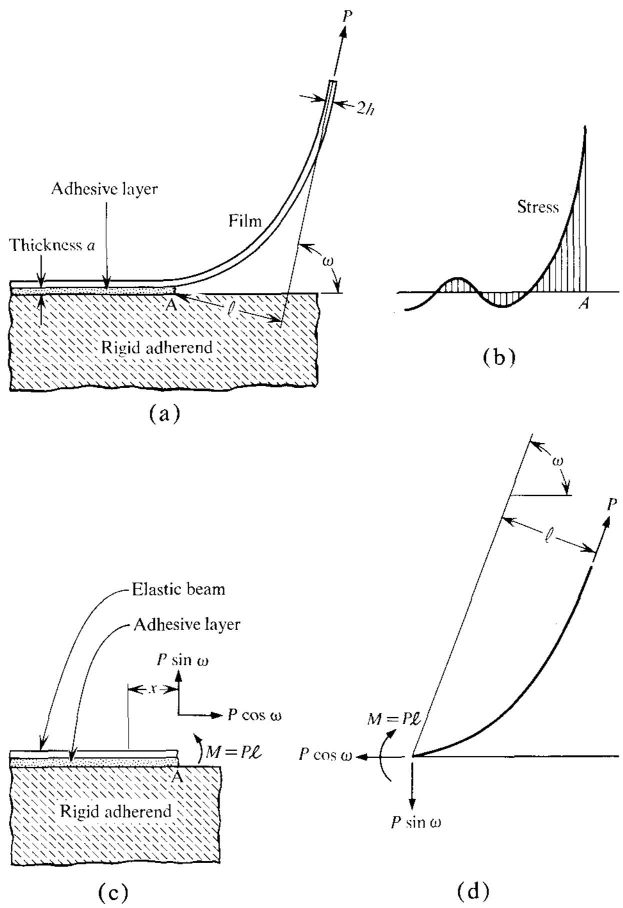

Figure 2 (a) Schematic diagram of peeling; (b) stress distribution in adhesive layer near point of cleavage; (c) bonded part (beam on elastic foundation); (d) free part (elastica).

The adhesive interlayer stress is

$$\sigma = yY/a. \quad (2)$$

Note that the stress σ varies in a damped oscillatory form as shown in Fig. 2(b).

The moment M is related to the force P by integrating the elastica equation for the free flexible part of the infinitely long strip [Fig. 2(d)]. The moment M is found to be related to the force P by

$$M = [2PEI(1 - \cos \omega)]^{1/2}. \quad (3)$$

Substitution of (3) into (1) and (2) leads to a relation between peel force P and the adhesive interlayer stress. The maximum stress in the adhesive occurs at $x = 0$:

$$\sigma_c = (Y/2\beta^3 EIa)\{\beta[2PEI(1 - \cos \omega)]^{1/2} + P \sin \omega\}.$$

In the usual experimental setup, the peel force is directed perpendicular to the film, so that $\omega = 90°$, and the cleavage stress of the adhesive is

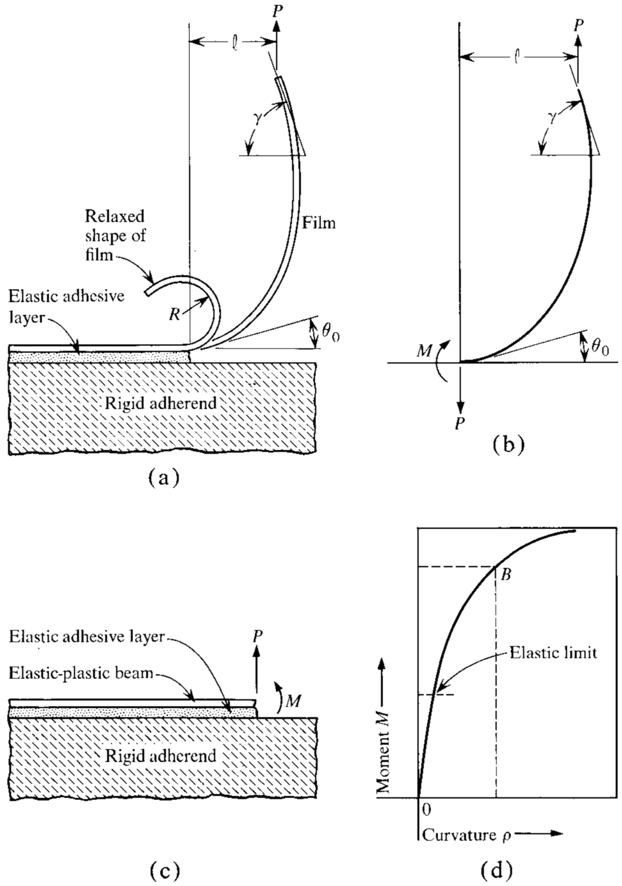

Figure 3 (a) Schematic diagram of 90° peel and relaxed shape of peel-film; (b) free portion (elastica with initial curvature); (c) elastic-plastic beam on elastic foundation; (d) moment-curvature diagram.

$$\sigma_c = (Y/2\beta^3 EIa)[\beta(2PEI)^{1/2} + P]$$
$$= (2YP/ab)^{1/2} + 2P\beta/b; \tag{4}$$

i.e.,

$$P/b = (Y/4a\beta^2)\{1 + (2\sigma_c\beta a/Y) - [1 + (4\sigma_c\beta a/Y)]^{1/2}\}. \tag{5}$$

• *Elastic-plastic theory*

Suppose that at some point the stresses in the film have exceeded the elastic range. The moment curvature relation for bending of the film can be found from the stress-strain relation. In the vicinity of the cleavage point, the film has been overstressed. Suppose the radius of curvature and moment of the overstressed beam (film) at the cleavage point are ρ and M, respectively. If the film at this portion is allowed to relax, it would assume a relaxed radius of curvature R, where

$$\frac{1}{R} = \frac{1}{\rho} - \frac{M}{EI}. \tag{6}$$

The steady-state assumption implies that every point in the free flexible portion has been overstressed in the same manner as that section in the vicinity of the cleavage point. If the flexible portion is allowed to relax, it would assume a constant radius of curvature R. Note that one can no longer assume that the force P acts along the tangent of the pulled end of the strip. Let the angle there be γ, and also let the angle between the cleaved end and the horizontal be θ_0. Consider the free portion as an elastica with initial curvature [Fig. 3(b)]. It turns out that one could still integrate the elastica equation for an initially curved beam (Appendix A) to obtain the relation between force P and moment M:

$$P(\sin\gamma - \sin\theta_0) = M\left(\frac{M}{2EI} + \frac{1}{R}\right). \tag{7}$$

Combining Equations (6) and (7) yields

$$P(\sin\gamma - \sin\theta_0) = M\left(\frac{1}{\rho} - \frac{M}{2EI}\right). \tag{8}$$

But the moment M and radius of curvature ρ are uniquely defined by the beam dimensions and the stress-strain relationship. Every point on the M-ρ diagram in Fig. 3(d) corresponds to a unique value of P $(\sin\gamma - \sin\theta_0)$. The angle γ has to be solved from the length of the free strip. We define

$$\alpha \equiv \sin\gamma - \sin\theta_0. \tag{9}$$

Upon physical grounds, we know that α is often approximately equal to but a little less than 1.

We shall assume that α is known and equal to 1; then for any moment M, one can find the force P that represents the applied load in the problem of an elastic-plastic beam on an elastic foundation as shown in Fig. 3(c).

Details of how to find the cleavage stress in the adhesive interlayer by analyzing the model of an elastic-plastic beam on an elastic foundation are outlined in Appendix B. The basic idea is to replace the section of the moment-curvature diagram OB by a bilinear characteristic curve. The resulting equations are nonlinear, and are solved by an iteration procedure. Again, the adhesive cleavage stress is obtained from the beam deflection at the cleavage point by using Winkler's foundation theory. Thus, for any point on the moment-curvature curve, one can find the values of the peel force P and the cleavage stress σ_c. With this method, a graph of P vs σ_c can be constructed. The peel force corresponding to any particular value of cleavage stress can be evaluated by interpolation.

• *Elastic-plastic adhesives*

The analysis as described is applicable for a brittle elastic adhesive, i.e., an adhesive whose stress varies in proportion to its strain until rupture occurs. Many adhesives are not so elastic and a means for approximating an actual complete behavior with an elastic representation is desirable. Suppose that the strain energy density of the adhesive material is a valid index of its contribution to peeling resistance. Then an artificial elastic modulus can be substituted, which when effective over the true strain will produce the true strain energy density (area under the stress-strain curve). (The true ultimate stress or the true modulus could have been maintained instead of the true strain.)

Figure 4 is a typical stress-strain graph with some equal strain energy density elastic representations superimposed. The elastic modulus associated with each of the straight-line approximations and the corresponding calculated peel forces for like films are shown. The near equality of calculated forces suggests that strain energy density is indeed an index of the adhesive contribution to peeling resistance. It further suggests that the straight-line representation of the adhesive is a reasonable approximation of the true elastic-plastic relationship. Accordingly, the authors suggest that in the case of a non-brittle adhesive, one employ an artificial modulus and an ultimate stress as input parameters to the analysis, based upon the actual strain energy density and actual ultimate strain as outlined earlier.

• *Computer program*

A computer program* has been written that incorporates the various steps discussed in this section and also in Appendices A and B. The program simulates the 90° peel test, and will give the peel force corresponding to the input cleavage stress of the adhesive. The inverse process, computation of cleavage stress from a knowledge of the peel force involves but a trivial modification of the program.

Experimental procedure

While verification of the analytical model was attempted largely by comparing our results with measurements made by others, a limited experimental effort of our own was undertaken. In making 90° peel force measurements the angle is maintained at about 90°, but a deviation of ±5° does not affect peel force appreciably, as indicated in the measurements by Beaudouin [31]. For the tests described in this paper, the forces were recorded over a maximum peel distance of about four inches, divided equally on both sides on the center line of an Instron tensile load cell, which was positioned a minimum of 22 inches above the sample (Fig. 5). A light tension member is pivotably attached at both the load cell end and at the end of the peel strip. A 0.002 in. thick, 1.0 in. wide spring steel strip was used for the tests and attached to the end of each specimen by means of flexible adhesive tape.

The minimum length of the free (separated) portion, when measurements are started, is sufficient that the

*The computer program is experimental and is not available outside the IBM Corporation.

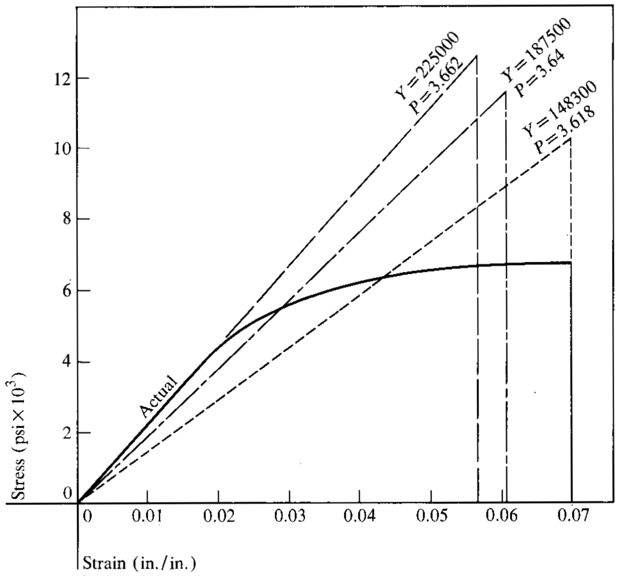

Figure 4 Equal-energy approximations of adhesive behavior.

Figure 5 Sketch of experiment.

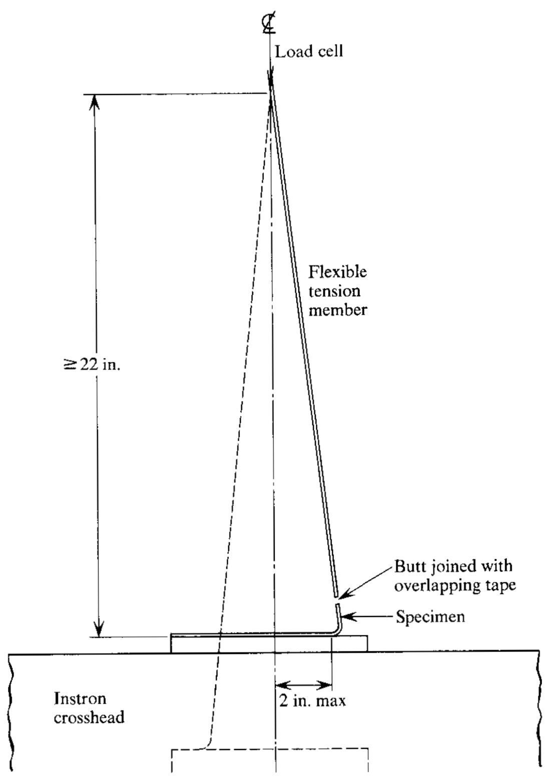

slope at the end is essentially in the direction of the applied force. In cases where the peel film is not stressed above the elastic limit, a length*

$$L \geq \left(\frac{5E\ bh^3}{6P}\right)^{1/2}$$

would be adequate where E is Young's modulus, b is width, h is thickness of the strip and P is the peeling force. In the usual case, where the film is overstressed, the corresponding length based on the elastic limit of the strip material would be sufficient. This works out to

$$L \geq 2.24 \frac{Eh}{y},$$

where y is the elastic limit of the material.

The measurements were made with free ends exceeding the length calculated for the overstressed strip. Peel force was measured at various peeling rates to insure that viscous behavior was not significantly influencing the results.

At first, Instron measurements were interpreted by averaging the peel force over an entire peel distance-force integral. (The Instron chart included reversal to unload the cell without separating the film.) Later, when it was realized that the history of the peeling strip stress influenced peel measurement, early portions of the curves were ignored and only the average values of apparent steady-state behavior were considered as representative peel force.

• *Example*

(a) Experimental

A single strip of blued spring steel (AISI C-1095) heat treated to RC 48-51 was procured for this experiment. The dimensions of the strip were 0.002 in. thick by 1.0 in. wide. After the strip was divided into halves, one of the halves was hydrogen annealed, giving it a yield strength of 33×10^3 psi and an ultimate strength of 66×10^3 psi (compared to the corresponding values of 207×10^3 psi and 283×10^3 psi for the hard sample). The hard portion was lightly etched in hydrochloric acid to remove the blue oxide coating. The soft part, from which the coating was removed in the annealing process, was subjected to the same etch so that the surfaces of both portions would be alike. This process yielded two peel strip samples which were alike with respect to modulus of elasticity, dimensions, material and surface. The only significant differences were in yield strength and behavior at stresses above the yield strength.

*Interpolation between solutions for the elastica problem [32] yields $L - \Delta$ (our R) $= 0.445L$ for $L = \left(\frac{10\ EI}{P}\right)^{1/2} = \left(\frac{5\ bh^3}{6P}\right)^{1/2}$ or $R = \left(\frac{1.98\ EI}{P}\right)^{1/2}$, whereas for $L = \infty$, $R = \left(\frac{2\ EI}{P}\right)^{1/2}$.
Maximum error for the moment arm R is then 0.5%.

Table 1 Peel force as a function of peeling rate for annealed and hardened steel strips 0.002 in. thick, bonded with 0.0035 in. of 3M 1838 adhesive.

	Peel force (lbs)					
	Hardened			*Annealed*		
Peeling rate (in./min.)	*Hi*	*Lo*	*Av*	*Hi*	*Lo*	*Av*
0.002						
0.01		0.93				
0.1*			0.75	1.65	1.28	1.44
0.2	0.80	0.40	0.62	1.44	1.04	1.18
0.5	0.67	0.35	0.59			
1.0			0.84			
5.0*	0.88	0.70	0.77	1.36	1.10	1.23
10.0*	0.73	0.54	0.63	1.54	1.14	1.34
Computed force			0.79			1.53

*Annealed steel strips were not surface-etched.

These strips were cut into 5 in. lengths and bonded to 0.250 in. thick ground steel plates with Scotch-Weld* 1838 adhesive controlled to 0.0035 in. thickness. Four strips were bonded to each plate, with hard strips interspersed with soft ones so as to avoid differences in curing and conditioning. The samples were cured for 30 minutes at 250°F and stored in a 70°F, 40% RH environment for a minimum of three days before peel strength was measured.

The results of the peel strength measurements are given in Table 1. After peeling, the strips of the hardened steel relaxed to flat or slightly curved forms, indicating that they had not, or had just barely, exceeded the yield strength of the material. The soft strips relaxed to a radius of about 0.31 in. except in the region adjacent to the cleavage line, where the radius was about 0.08 in. This shows that the material was overstressed in bending before cleavage and again overstressed in straightening subsequent to cleavage. An attempt to measure the radius in the loaded condition during peeling yielded values of about 0.05 in. for the soft samples and 0.11 in. for the hard samples.

(b) Computation

The data needed for simulating peeling the same strip of annealed spring steel bonded by a brittle adhesive to a steel plate are as follows:

Adhesive thickness, $a = 0.0035$ in.;
adhesive tensile modulus, $Y = 98{,}500$ psi†;
adhesive cleavage stress, $\sigma_c = 6{,}900$ psi†; and
film width, $b = 1$ in.

*Registered trademark, Minnesota Mining and Manufacturing, Co., St. Paul, Minnesota.

†These are adjusted values which reflect real ultimate strain and strain energy density of some samples of 3M-1838 adhesive based on a private communication with C. K. Lim and M. A. Acitelli.

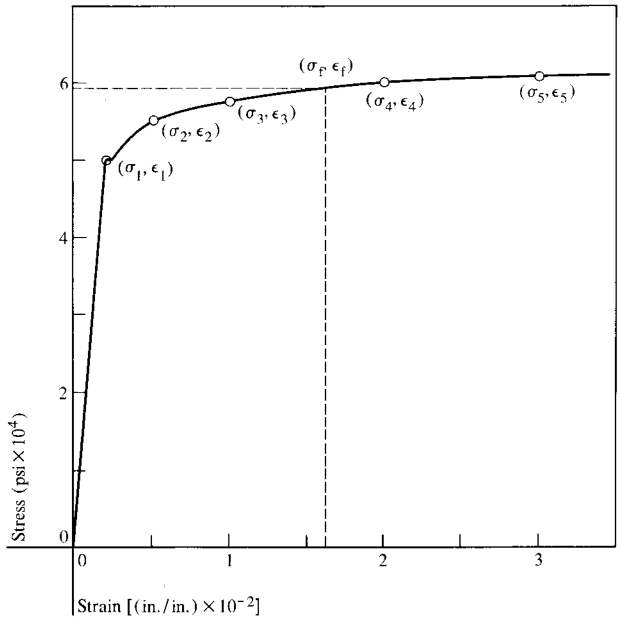

Figure 6 Stress vs strain from experiment.

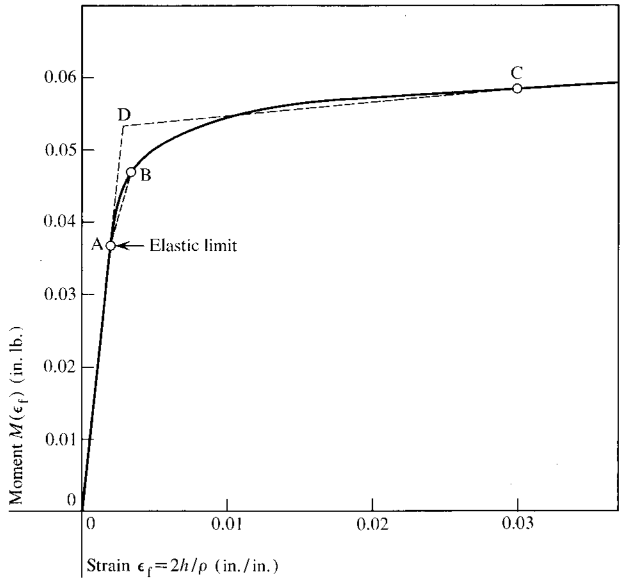

Figure 7 Moment vs strain computed from experimental data.

Figure 8 Peel force vs cleavage stress, calculated from the theory for the experimental materials.

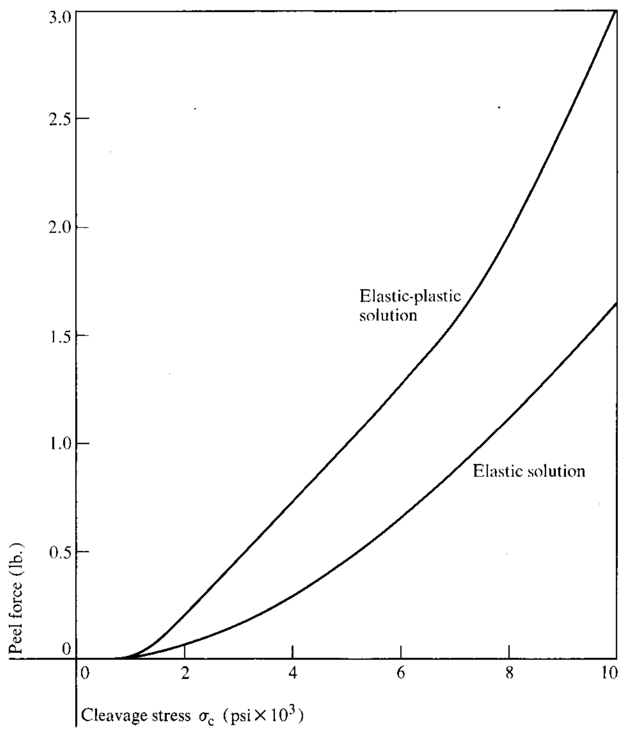

The film stress-strain data taken directly from a tensile test are:

stress:	50,000	55,000	57,500	60,000	61,000	psi
strain:	0.001667	0.005	0.01	0.02	0.03	in./in.

A plot of the tensile stress-strain relation is shown as the solid line in Fig. 6. A moment curvature plot of the steel strip based upon this set of data is plotted in Fig. 7. These are the intermediate results from our computer program.

The relation between peel force and cleavage stress is plotted in Fig. 8. The peel force corresponding to the elastic-plastic theory is 1.53, and that corresponding to the elastic theory is 0.79. The former is found by interpolation. Table 1 gives a comparison of the computed results with some experimental results.

The good agreement between theory and experiment may be fortuitous, considering the wide scatter usually encountered in peel tests; nevertheless the present elastic-plastic theory gives a reasonable estimate of the peel force from the physical properties of the adhesive and the film. Computer runs have been made for many other examples, and some observed trends in the results are included below.

Conclusions

Peeling of a properly bonded film from a compliant underlayer has been analyzed. The analysis has been described and quantitatively relates peeling force to the mechanical properties of a thin elastic layer attached to a rigid substrate. It takes into account the nonlinear as well as the linear behavior of the peel film. Also, a means is suggested for adjusting the elastic layer parameters to approximately duplicate the complete stress-strain behavior of an adhesive material.

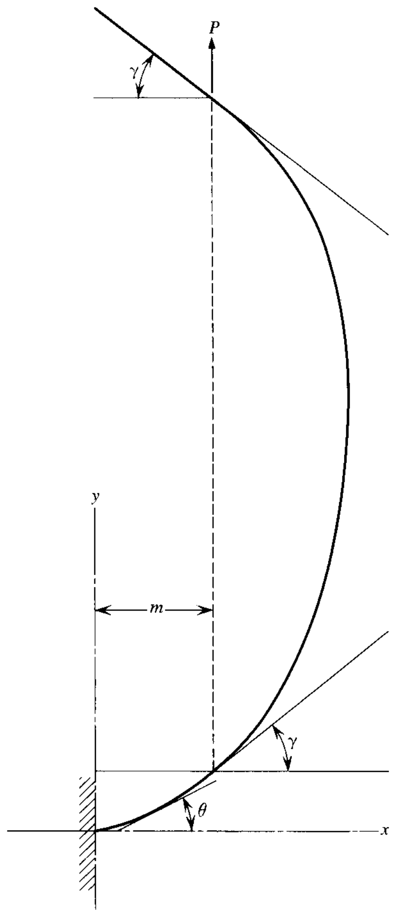

Figure A-1 Loaded shape of initially curved, inextensible bar.

Examination of the results from computer programs for a number of examples indicates the following relationships:

1. Within the context of thin layers, an increase in adhesive thickness is accompanied by an increase in resistance to peeling. However, as the adhesive becomes thick, the rate of increase in resistance to peeling becomes smaller.
2. There is often a particular thickness of peel film which exhibits higher resistance to peeling than greater or lesser thicknesses.
3. Peeling force is relatively insensitive to the stress-strain relationships of an adhesive, as long as their total integral, which represents strain energy density to rupture, remains constant.
4. Resistance to peeling increases with the onset of yielding of the peel film in bending. That is, if two adhesive systems are identical except for yield strength of the film, the film that yields will resist a greater peel force.

While not all of the analytical results have been tested experimentally, the first and fourth of the above have been supported by experimental data. Spies [15] and Mylonas [22] have reported observations similar to our second result.

It has been experimentally observed that in some adhesive systems, peeling force becomes minimum at some finite peeling rate.

Peel force measurements obtained by different testing methods cannot be directly compared with each other. The 90° peel test from a rigid foundation is the most universally applicable testing means and, so far, the most predictable from material properties and geometry.

The susceptibility to failure of a bond depends not only on its resistance to peeling force, but also on the resistance of the adherends to conform to each other, i.e. a film with a very low stiffness will not be likely to transmit a large moment at a possible cleavage site.

A logical extension from this paper is the application of a more nearly exact foundation theory. Then the effect of greater thickness of the underlayer can be analyzed and the effects of the adhesive near the edges of a peel strip can be considered.

Acknowledgments

The authors acknowledge the assistance of the following individuals in this work: M. A. Acittelli, C. K. Lim, D. W. Rice, A. L. Jones, J. S. Drotar, and H. G. Houghtalen.

Appendix A: relation between peeling moment and peeling force

Consider an initially curved inextensible bar whose free shape is given by $\eta = \eta(s)$, and whose loaded shape is given by $\theta = \theta(s)$ (Fig. A-1). If the bar is of constant flexural rigidity acted upon by a force P in the $(+y)$ direction, the function θ is governed by

$$EI\,\frac{d^2\theta}{ds^2} + P\cos\theta = \frac{d^2\eta}{ds^2}\,. \tag{A-1}$$

If this bar has constant initial curvature $1/R$,

$$\frac{d\eta}{ds} = \frac{1}{R},\ \frac{d^2\eta}{ds^2} = 0. \tag{A-2}$$

Integrating (A-1), we have

$$\frac{1}{2}\left(\frac{d\theta}{ds}\right)^2 = -\frac{P}{EI}\sin\theta + C. \tag{A-3}$$

At $x = m$, $\theta = \gamma$, $d\theta/ds = 1/R$. The integration constant C is

$$C = \frac{1}{2}\left(\frac{1}{R}\right)^2 + \frac{P}{EI}\sin\gamma. \tag{A-4}$$

Substitution of (A-4) into (A-3) gives

$$\left(\frac{d\theta}{ds}\right)^2 = \frac{2P}{EI}(\sin\gamma - \sin\theta) + \frac{1}{R^2}\cdot \tag{A-5}$$

At $x = 0$, $\theta = \theta_0$, and the bending moment at that point is $M = Pm$. The curvature at that point is

$$\frac{d\theta}{ds} = \frac{1}{R} + \frac{Pm}{EI}\cdot \tag{A-6}$$

Substituting (A-6) into (A-5) yields

$$\frac{1}{R} + \frac{Pm}{EI} = \frac{2P}{EI}(\sin\gamma - \sin\theta_0) + \frac{1}{R^2}\cdot \tag{A-7}$$

After some algebraic manipulation, one has

$$M = -\frac{EI}{R} + \left[\left(\frac{EI}{R}\right)^2 + 2PEI(\sin\gamma - \sin\theta_0)\right]^{1/2}. \tag{A-8}$$

If $R = \infty$, then $\gamma = \pi/2$, and $\theta_0 = 0$, and the result simplifies to

$$M = (2PEI)^{1/2}. \tag{A-9}$$

This equation relating peel moment to the peel force for initially straight film may be found in Kaelble's paper [17].

Equation (A-7) may be rewritten as

$$P(\sin\gamma - \sin\theta_0) = \frac{M^2}{2EI} + \frac{M}{R}\cdot \tag{A-10}$$

Experimental observation shows that the angles γ and θ_0 are very close to $\pi/2$ and zero, respectively, although their exact values are not known. For practical purposes we assume

$$\alpha \equiv \sin\gamma - \sin\theta_0 = 1. \tag{A-11}$$

Appendix B: determination of cleavage stress in the adhesive

• *Moment-curvature relation*

Figure 6 is a typical stress-strain diagram for steel. Other materials such as copper and aluminum behave in similar manner. In practice, it is convenient to select n points on the stress-strain diagram and represent the inelastic behavior of the material by straight lines drawn between the points. If the first point is always the elastic limit, then the material behavior is completely defined by the matrix

$$\begin{pmatrix} \sigma_0, \sigma_1, \sigma_2, \sigma_3 \cdots \sigma_n \\ \epsilon_0, \epsilon_1, \epsilon_2, \epsilon_3 \cdots \epsilon_n \end{pmatrix},$$

where $\sigma_0 = \epsilon_0 = 0$. In Fig. 6 for example, $n = 5$.

The stress σ corresponding to any strain ϵ, $\epsilon_K > \epsilon > \epsilon_{K-1}$, is given by

$$\sigma = \sigma_{K-1} + E_K(\epsilon - \epsilon_{K-1})$$

$$\text{where } E_K = \frac{\sigma_K - \sigma_{K-1}}{\epsilon_K - \epsilon_{K-1}}. \tag{B-1}$$

The moment sustained by a rectangular beam of cross-section bh is

$$M = 2b\int_0^{h/2} \sigma y dy. \tag{B-2}$$

In the beam the maximum stress and strain occur at the outer fiber, denoted as (σ_f, ϵ_f). Then, the moment corresponding to (σ_f, ϵ_f) is

$$M(\epsilon_f) = \frac{h^2 b}{2\epsilon_f^2}\left\{\frac{1}{3}E_1\epsilon_1^3 + \sum_{i=2}^{i_f}\left[\frac{1}{2}(\sigma_{i-1} - E_i\epsilon_{i-1})(\epsilon_i^2 - \epsilon_{i-1}^2) + \frac{1}{3}E_i(\epsilon_i^3 - \epsilon_{i-1}^3)\right]\right\}. \tag{B-3}$$

The moment-curvature diagram for the material in Fig. 6 with $h = 0.002$, $b = 1$ is shown as the solid line in Fig. 7. Note that it is a smooth curve, although the stress-strain diagram upon which it is based is made up of straight lines joined together.

• *Elastic-plastic beam on elastic adhesive layer*

Suppose that a semi-infinite beam whose moment-curvature behavior is similar to that in Fig. 7 is overlaid on a Winkler foundation representing the adhesive layer, and subjected to force and moment at the end of the beam as shown in Fig. B-1(a). Little is known as to how to approach this problem by means of the exact moment-strain relation as in Fig. 7.

In the physical problem the applied moment is very close to the maximum moment, so that one knows a priori what region of the curve in Fig. 7 will be involved. Suppose one knows that the plastic region will be the solid curved line AB. Then that part can be approximated by the dotted straight line AB in Fig. 7. If the plastic region involved is instead the solid curved line ABC, a good approximation would be the dotted lines AD and DC. The slope of DC can be set as the slope at the midpoint of the projection of AC on the abscissa. In this manner an approximate bilinear representation to the moment-strain curve is obtained. The exact formulation of the elastic-plastic beam on a Winkler foundation in Fig. B-1(a) is replaced by the approximate formulation shown in Fig. B-1(b). To the left of J the beam obeys the lower linear relations in the moment-curvature curve. From J to the right end of the beam the moment-curvature relation is goverened by the upper linear relation in Fig. B-1(b). The position of J is found from the condition that the moment there is equal to M_J. Denote

E = Young's modulus of beam associated with the lower characteristic,

E_1 = Young's modulus of beam associated with the upper characteristic,

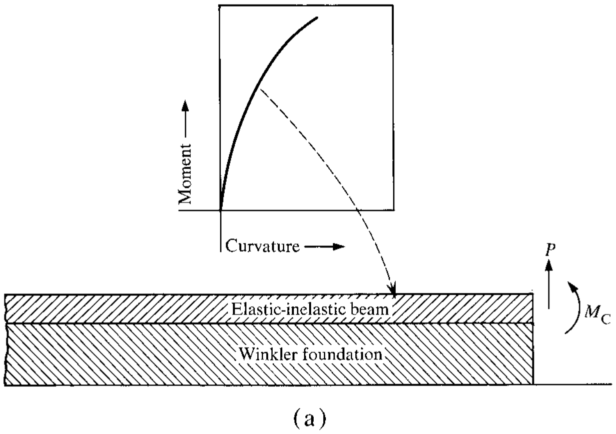

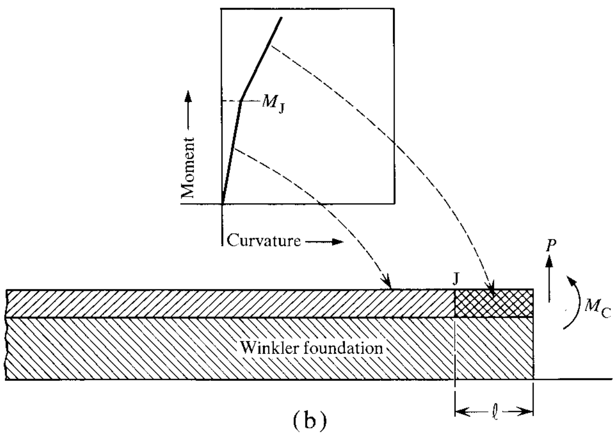

Figure B-1 Semi-infinite beam on Winkler foundation, subjected to force and moment. (a) Exact representation; (b) approximate representation for determining cleavage stress.

b = width of beam,
h = height of beam,
Y = Young's modulus of adhesive,
a = thickness of adhesive,
$\beta = (3Yh/E_1a)^{1/4}$,
$\gamma = (E_1/E)^{1/4}$,
$I = 2M_J/Ybh^2$,
$K = 2M_C/Ybh^2$,
$F = -2P/Ybh$, and
$\phi = \ell/h$.

The condition that the moment at J is equal to M_J, while the applied moment and force at the end are M_C and P, may be shown to be equivalent to the requirement that

$$F\beta = e^{\beta\phi}[(B-A)\cos\beta\phi - (B+A)\sin\beta\phi] + e^{-\beta\phi}[(D+C)\cos\beta\phi - (C-D)\sin\beta\phi], \quad \text{(B-4)}$$

where A, B, C, and D are found from

$$(1-\gamma)A + B - (1+\gamma)C + D = \gamma^3\beta^2 I;$$
$$B \qquad - D = \beta^2 I;$$
$$(1-\gamma)A + \gamma B + (1+\gamma)C + \gamma D = \gamma^2\beta^2 I;$$
$$(-e^{\beta\phi}\sin\beta\phi)A + (e^{\beta\phi}\cos\beta\phi)B + (e^{-\beta\phi}\sin\beta\phi)C - (e^{-\beta\phi}\cos\beta\phi)D = \beta^2 K. \quad \text{(B-5)}$$

The unknown quantity ϕ is found from the above relation by an iterative procedure. The cleavage stress in the adhesive is found from the deflection at the end of the beam. It was found to be

$$\sigma_c = Y\{(e^{\beta\phi}\cos\beta\phi)A + (e^{\beta\phi}\sin\beta\phi)B + (e^{-\beta\phi}\cos\beta\phi)C + (e^{-\beta\phi}\sin\beta\phi)D\}. \quad \text{(B-6)}$$

In summary, for some load combination P and M_C, one finds an approximate bilinear representation of the nonlinear moment-curvature curve. The next step is to determine the value of ϕ that will satisfy (B-4) and (B-5). The cleavage stress associated with the load P and M_C is calculated from (B-6).

Note added in proof:
Some recent works on adhesion have been reported at the symposium, "Recent Advances in Adhesion—1971" held at the American Chemical Society Meeting in Washington, D.C., September 1971. Particularly relevant to the work here is the paper, "The Effects of Plasticity in Adhesive Fracture" by M.-D. Chang, K. L. DeVries and M. L. Williams, which was preprinted in *Am. Chem. Soc. (162nd Meeting), Organic Coatings and Plastic Chemistry Div.*, Vol. 31, No. 2, September 1971.

References

1. D. D. Eley, ed., *Adhesion*, Oxford University Press, London 1961.
2. P. Weiss, ed., *Adhesion and Cohesion*, Elsevier, Amsterdam 1962. (*Proc. Symposium on Adhesion and Cohesion*, General Motors Research Laboratory, Detroit, Michigan 1961).
3. M. J. Bodnar, ed., *Symposium on Adhesives for Structural Application*, John Wiley and Sons, New York 1962 (symposium held at Picatinny Arsenal, New Jersey, 1961).
4. *Symposium on Adhesion*, ASTM Spec. Tech. Publ. 360, Philadelphia 1964.
5. M. J. Bodnar, ed., *Structural Adhesive Bonding*, Applied Polymer Science Symposium No. 3, Interscience, New York 1966.
6. R. Houwink and G. Salomon, eds., *Adhesion and Adhesives*, Vols. 1 (Adhesives) and 2 (Applications), 2nd revised edition, Elsevier, Amsterdam 1967.
7. D. Satas, ed., *Conference on Adhesion of Polymers*, Wayne State University 1967.
8. R. Patrick, ed., *Treatise on Adhesion and Adhesives*, Vols. 1 and 2, Marcel Dekker Inc., New York 1968.
9. J. J. Bikerman, *The Science of Adhesive Joints*, 2nd edition, Academic Press, New York 1968.
10. D. D. Eley, ed., *Adhesion—Fundamentals and Practice*, Maclaren & Sons, London 1969. (Report of an International Conference held at Nottingham, England September, 1966.)

11. D. J. Alner, ed., *Aspects of Adhesion—5*, CRC Press, Cleveland 1969.
12. D. H. Kaelble, *Physical Chemistry of Adhesions*, John Wiley and Sons, New York 1971.
13. P. A. Jacquet, *J. Electrochem. Soc.* **66,** 393 (1964).
14. R. J. Chadwick, *J. Inst. Metals* **62,** 277 (1968).
15. G. J. Spies, *J. Aircraft Eng.* **25,** 64 (1953).
16. J. J. Bikerman, *J. Appl. Phys.* **28,** 1484 (1957).
17. D. H. Kaelble, *Trans. Soc. Rheology* **3,** 161 (1959).
18. D. H. Kaelble, *Trans. Soc. Rheology* **4,** 45–73 (1960).
19. C. Jouwersma, *J. Polymer Science* **65,** 253 (1960).
20. S. Yurenka, *Symposium on Adhesives for Structural Application*, John Wiley and Sons, New York 1962, pp 15–24.
21. E. B. Saubestre, L. J. Durney, J. Hajdu, and E. Bastenbeck, *Plating* **52,** 982 (1965).
22. C. Mylonas, "Analysis of Peeling", *4th Int. Congress on Rheology*, 423–447 (1961).
23. D. H. Kaelble, *Trans. Soc. Rheology* **9,** 2, 135 (1965).
24. D. H. Kaelble, *J. Adhesion* **1,** 102 (1969).
25. D. H. Kaelble, *Trans. Soc. Rheology* **15,** 275 (1971).
26. D. H. Kaelble and R. S. Reylek, *J. Adhesion* **1,** 124 (1969).
27. J. D. Burton, W. B. Jones, and M. L. Williams, *Trans. Soc. Rheology* **15,** 39 (1971).
28. H. N. Vazirani, "How to Monitor Joint Quality with a Peel Resistance Test", *Adhesive Age* **13,** 1, 40 (1970).
29. A. J. Duke, and R. P. Stanbridge, *J. Appl. Polymer Sci.* **12,** 1487 (1968).
30. M. Hetényi, *Appl. Mech. Review* **19,** 95 (1966).
31. P. L. Beaudouin, "Measurement of the Adhesion of Thin Metal Films to their Substrates," *Technical Report 22. 1060*, IBM Corp., E. Fishkill, New York.
32. K. E. Bisshop and D. C. Drucker, *J. Quart. Appl. Math* **3,** 272 (1945).

Received July 16, 1971

W. T. Chen is with the IBM Systems Development Division and T. F. Flavin, the Components Division; both authors are located at the IBM Laboratory, Endicott, New York 13760.